Partially disordered state with short-range spin correlation in $S = 5/2$ classical triangular antiferromagnet Ag_2FeO_2

H. K. Yoshida,[1,2,*] M. Matsuda,[3] M. B. Stone,[3] C. R. dela Cruz,[3] T. Furubayashi,[1] M. Onoda,[1] E. Takayama-Muromachi,[1] and M. Isobe[1]

[1]*National Institute for Materials Science (NIMS), Namiki, Tsukuba, Ibaraki 305-0044, Japan*
[2]*Department of Physics, Faculty of Science, Hokkaido University, Sapporo, Hokkaido 060-0810, Japan*
[3]*Neutron Scattering Division, Oak Ridge National Laboratory (ORNL), Oak Ridge, Tennessee 37831, USA*

(Received 10 July 2020; revised 17 September 2020; accepted 19 October 2020; published 10 November 2020)

A triangular-lattice antiferromagnet of Ag_2FeO_2 was synthesized under high pressure. Its magnetism was studied in terms of electrical resistivity, magnetic susceptibility, heat capacity, powder neutron scattering, and Mössbauer spectroscopy. The magnetic state of Ag_2FeO_2 changes successively through a second-order phase transition at $T_p = 36$ K and a crossover at $T_c = 20$ K. A partially disordered (PD) state appears below T_p, in which $\approx 2/3$ spins are ordered and the remaining $\approx 1/3$ spins fluctuate, which state persists at least down to 5 K. The spin correlation length starts to grow at T_p; however, it remains very short (≈ 27 Å) below T_c. This exotic magnetism is concerned with strong frustration in the classic antiferromagnetic triangular lattice.

DOI: 10.1103/PhysRevResearch.2.043211

I. INTRODUCTION

The ground state (GS) of frustrated antiferromagnets has been intensively studied in condensed matter physics. The most important and fundamental issue has been to understand how the macroscopic degeneracy caused by the frustration is released by forming a unique state at low temperature. According to theories, the magnetic states of classical triangular antiferromagnets (TAFMs) depend on the anisotropy of spins. It is well known that the Ising spin system does not exhibit a long-range order (LRO) down to 0 K [1,2]. In the XY and Heisenberg spin systems, the GS has a 120° LRO. However, its ordering process is quite model dependent. For example, in the XY model, the chirality and the Kosterlitz-Thouless (KT) transition occur sequentially at finite temperatures [3,4]. In the Heisenberg model, the paired to unpaired transition of the Z_2 vortices occurs [5].

However, finding an appropriate material for testing these theoretical predictions is a challenging task. Actual TAFMs possess certain undesirable factors such as three-dimensionality, structural distortion, and ion disorder, which always mask the essential properties of frustrated magnets. Therefore, ideal model compounds are desired for understanding of the intrinsic magnetism of classical TAFMs.

Ag_2MO_2 (M = transition metal) may have some potential for use as an ideal system for the study of the magnetic properties of TAFMs [6]. The crystal structure of Ag_2MO_2 consists of alternate stacks of $M^{3+}O_2$ and $(Ag_2)^+$ layers. The former includes a triangular lattice of M^{3+} ions, whereas the latter provides itinerant electrons from the quarter-filled Ag 5s band. Because there is no superexchange pathway between adjacent MO_2 layers, this system can be regarded as an ideal two-dimensional TAFM.

In previous work, M = Mn (d^4 high spin $S = 2$) and Ni (d^7 low spin $S = 1/2$) model compounds of classical and quantum TAFM have been studied [7,8]. However, these elements exhibit a structural phase transition from R-3m to $C2/m$ at a finite temperature, because the orbital degree of freedom in the e_g level couples with the lattice degree of freedom. This kind of structural distortion may mask the essential properties of frustrated magnets and complicates the magnetic properties of the system.

In this paper, we report the exotic magnetic states in $S = 5/2$ classical TAFM Ag_2FeO_2. We succeeded in synthesizing Ag_2FeO_2 under high pressure. A prominent advantage of this system is that the magnetic frustration is not released through a coupling with other degrees of freedom, because the orbital momentum of the Fe^{3+} ion is quenched.

II. EXPERIMENTAL

Polycrystalline samples of Ag_2FeO_2 were prepared from a stoichiometric mixture of Fe_2O_3, Ag_2O, and Ag, using a high-pressure synthesis technique at 900 °C under 6 GPa. Using powder x-ray diffraction (XRD), the sample was confirmed to be predominantly a single phase of Ag_2FeO_2. The majority impurity is a small percentage of Fe_2O_3 (hematite). The electric resistivity and heat capacity were measured using a quantum design (QD) physical properties measurement system (PPMS). The magnetic susceptibility was also measured using QD magnetic property measurement system (MPMS). The powder neutron diffraction experiments were carried out

*Corresponding author: hyoshida@sci.hokudai.ac.jp

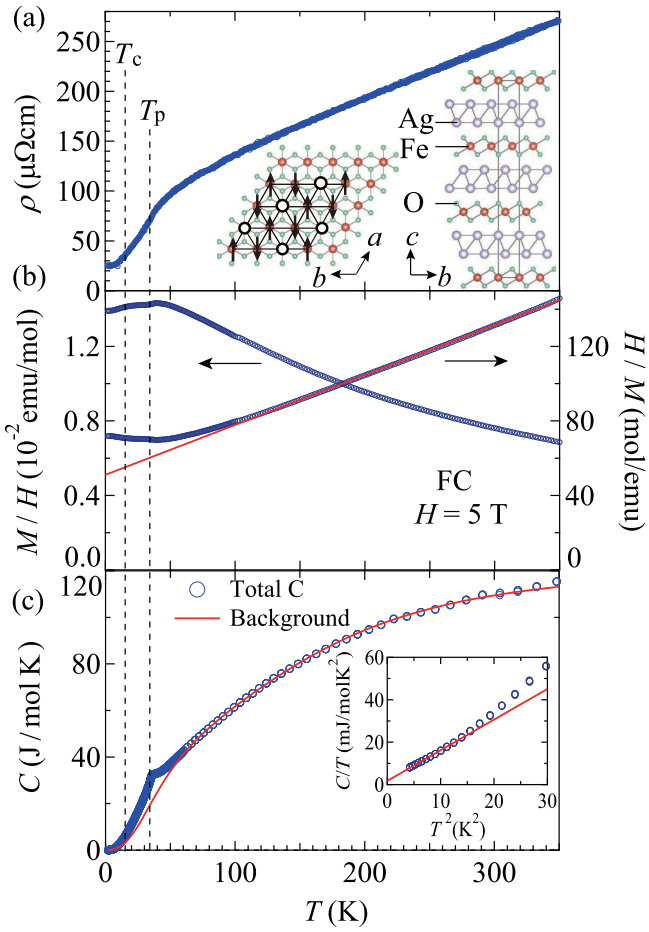

FIG. 1. Electrical resistivity (a), magnetic susceptibility (b), and heat capacity (c) of Ag_2FeO_2. In panel (a), the 3PD magnetic structure and the average crystal structure consists of alternating stacks of a triangular lattice of edge-shared FeO_6 octahedra and a double silver layer is illustrated. In panel (b), the red line indicates a linear fit to the inverse susceptibility. In panel (c), the solid curve shows the background heat capacity C_b. The inset of panel (c) is a C/T vs T^2 plot.

using the diffractometer HB-2A installed at high flux isotope reactor (HFIR) in Oak Ridge National Laboratory (ORNL). The neutron wavelength was fixed at $\lambda = 1.5373$ Å. The inelastic neutron scattering experiments were carried out on powder sample of Ag_2FeO_2 on the time-of-flight chopper neutron spectrometer ARCS [8], installed at the Spallation Neutron Source (SNS) at ORNL. We utilized an incident energy of 15 meV. The measurements were performed at 5 K using a closed-cycle refrigerator. The ^{57}Fe Mössbauer spectra were measured via transmission geometry using a ^{57}Co/Rh γ-ray source.

III. RESULTS

The XRD study revealed that the Bragg reflections of Ag_2FeO_2 was indexed with a trigonal (rhombohedral) Bravais lattice of $a = 2.9919(7)$ Å and $c = 25.013(5)$ Å. A structure model is illustrated in the inset of Fig. 1(a). The FeO_2 layer includes a Fe^{3+} ($3d^5$) equilateral triangular lattice. In the XRD profile, the Bragg peaks with indices of $h - k \neq 3n$ are

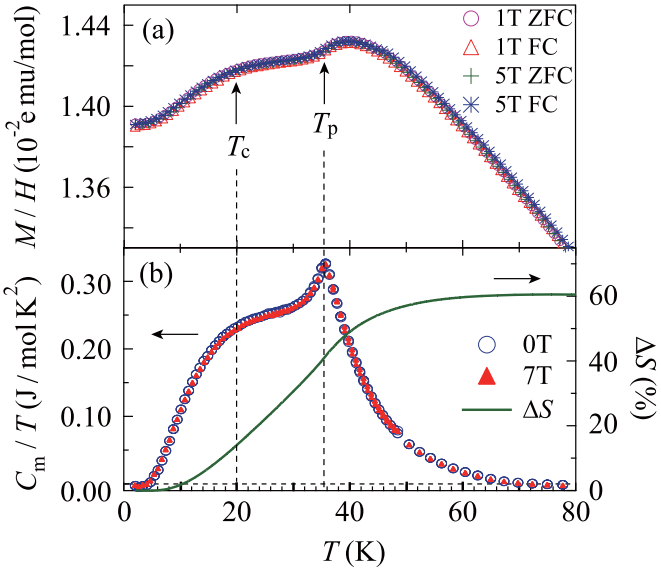

FIG. 2. (a) Temperature dependence of magnetic susceptibility below 80 K, measured at $H = 1$, 5 T in ZFC and FC conditions. (b) Magnetic heat capacity (C_m/T vs T plot) at $H = 0$, 7 T. The right axis indicates the estimated magnetic entropy (see text).

relatively diffuse, suggesting the existence of stacking faults in the crystal structure [9]. The detailed structure was studied using the profile-analysis method. The results are summarized in the Supplemental Material [10].

Ag_2FeO_2 exhibits metallic behavior down to 2 K, as shown in Fig. 1(a). A gradual decrease was observed around 40 K, corresponding to a magnetic anomaly at T_p. This decrease is presumably attributed to the suppression of the magnetic scattering of Ag 5s itinerant electrons, because Fe spins form an ordered state below T_p.

Figure 1(b) shows the temperature dependence of magnetic susceptibility χ and its inverse, from 350 to 2 K under $H = 5$ T in a field-cooled process. χ obeys the Curie-Weiss law. From the linear fitting to χ^{-1}, the effective paramagnetic moment $p_{\rm eff} = 5.49\ \mu_B$ and Weiss temperature $\Theta_W = -190$ K were determined. This effective moment is close to the spin-only value $p_{\rm eff} = 5.92\ \mu_B$ that is expected for a high-spin Fe^{3+} ion, implying that the Fe 3d electrons are localized in the triangular lattice.

Figure 2(a) is a magnified plot of the region of the χ-T data measured under $H = 1$ and 5 T in the field-cooled (FC) and zero-field-cooled (ZFC) processes below 80 K. χ is nearly independent of the magnetic field over the whole temperature range. Furthermore, there is no irreversible hysteresis between the FC and ZFC data sets. χ exhibits a round maximum at 40 K. Below 40 K, χ shows a successive decrease at $T_p = 36$ K and $T_c = 20$ K. Interestingly, the ratio of the decrease $[\chi(40\ \text{K}) - \chi(2\ \text{K})]/\chi(40\ \text{K}) \approx 0.014$ is much smaller than the theoretical value of 1/3 expected in typical powder antiferromagnets. Generally, the stacking fault affects the magnetic properties of two-dimensional frustrated antiferromagnets which induces a disorder of interlayer exchange magnetic interaction. On the other hand, the interplane interaction in Ag_2FeO_2 is mediated by the Ruderman-Kittel-Kasuya-Yosida (RKKY) type with 5s conduction electrons of Ag_2 layer, which depends on the

interlayer distance of magnetic triangular lattices. Importantly, the stacking fault does not change the interlayer distance along the c direction, which is evidenced by the sharp (0, 0, l) reflections. Therefore, the magnetic interaction along the c axis is irrelevant from the stacking fault. No sign of the spin-glass transition in this compound is another proof of the absence of the disordering interactions.

Figure 1(c) shows the temperature dependence of the heat capacity C; a peak was found at $T = 36$ K. This temperature agrees well with T_p in χ, suggesting that this peak is due to a magnetic transition. To extract the magnetic part C_m, we estimated the background contribution C_b by fitting the data above 100 K. We assume that C_b consists of an electronic component $C_{el} = \gamma T$ and a lattice component C_l; $C_b = C_{el} + C_l$. The Sommerfeld coefficient γ was estimated to be 1.47 mJ mol^{-1} K^{-2}, from the C/T versus T^2 plot [inset of Fig. 1(c)]. The lattice component was defined as $C_l = xC_{D_1} + (5 - x)C_{D_2}$ using the two-Debye-phonon model [11]. As shown in Fig. 1(c), the calculated background line C_b reproduces well the C versus T plot above 100 K.

An approximate residual magnetic contribution C_m was obtained by subtracting C_b from the total heat capacity C; in Fig. 2(b), the C_m/T versus T plot is presented. The anomaly at T_p is clearly visible and, more importantly, a broad shoulder is observed at around $T = 20$ K. This broad feature corresponds to the anomaly observed in the magnetic susceptibility at T_c. Because the heat capacity exhibits almost no field dependence, the origin of the broad feature at T_c is not a Schottky anomaly but rather a bulk magnetic phenomenon. Magnetic entropy calculated based on C_m is shown on the right axis in Fig. 2(b). The values are normalized using the magnetic entropy $S = R\ln(2S + 1) = 14.89$ J mol^{-1} K^{-1} for an $S = 5/2$ system. About 40% of the magnetic entropy is released below T_p.

Figure 3(a) shows the neutron diffraction data measured at low temperatures. The magnetic Bragg reflections that can be assigned to indices (1/3, 1/3, L) were observed below T_p. This result indicates that the magnetic structure has a periodicity of three in the a and b axes. The ratios of the intensities to the peak positions of all the Bragg reflections are essentially unchanged below T_p, suggesting that there is no magnetic structural change even below T_c.

The magnetic Bragg peaks develop with decreasing temperature. However, their peak widths are much broader than the width of the adjacent nuclear Bragg peak (0, 0, 6) even at 4 K, as shown in Fig. 3(a), implying that the magnetic correlation has a short coherence. The inset of Fig. 3(a) shows the temperature dependence of the spin correlation length ξ determined from the Lorentzian-type function, $I = I_0/[(1/\xi)^2 + Q^2]$. As temperature decreases, ξ starts to grow at T_p and reaches the finite value of ≈27 Å (≈9 lattice spacing in the ab plane) at T_c.

The possible magnetic structure models below T_p that can satisfy the threefold periodicity on the triangular lattice are the 120° structure, the up-up-down ferrimagnetic structure, and the partially disordered (PD) state [12,13]. However, the presence of the ferrimagnetic structure is unlikely, because no spontaneous magnetization was observed. As shown in Fig. 3(a), the magnetic model calculation, assuming the three sublattice PD (3PD) state with Ising anisotropy along the

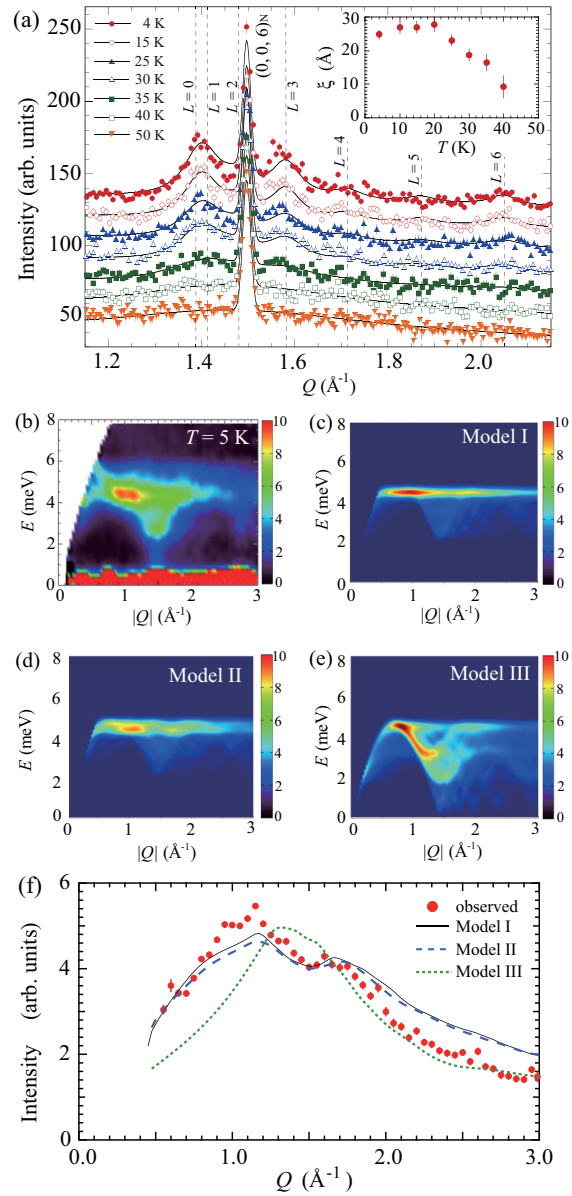

FIG. 3. (a) Nuclear (N) and magnetic Bragg reflections with indices of (1/3, 1/3, L) for neutron diffraction measured at various temperatures. The profiles are shifted at +15-count intervals. The black lines show the calculated diffraction pattern assuming the 3PD structure with $S \parallel c$. The inset shows the temperature dependence of the spin correlation length ξ. (b) Color contour map of the inelastic neutron scattering intensity $S(|Q|;E)$ for Ag_2FeO_2 powder sample measured with incident energy $E_i = 15$ meV at $T = 5$ K. Background signal measured using an empty cell was subtracted. The calculated excitation spectra of 3PD state with spin anisotropy $S \parallel c$ [(c), (d)] and 120° structure with $S \parallel ab$ plane (e). J_1, J_2, J_3, J_c, and D_c in the Hamiltonian (see text) are 5.1, 0.51, 2.6, 0, and −1.2 K (model I) for panel (c), 4.9, 0.49, 2.5, 0.8, and −1.2 K (model II) for panel (d), and 32.5, 0, 0, 0, and 5.9 K (model III) for panel (e), respectively. (f) Q dependences of the inelastic scattering intensity. Filled circles are intensities observed at 5 K integrated in the range of $3.5 \leqslant E \leqslant 6.0$ meV. Solid, broken, and dotted lines represent Q dependences of the calculated intensity integrated in the range of $3.5 \leqslant E \leqslant 6.0$ meV for panels (c) and (d) and $1.5 \leqslant E \leqslant 5.0$ meV for panel (e), respectively.

c axis and fitting the peak width and overall scale factor, reproduces the neutron diffraction pattern at all the measured temperature. This indicates that the 3PD structure is developed below T_p.

Inelastic neutron scattering spectrum provides firm evidence of the realization of the 3PD state. As depicted in Fig. 3(b), the clear magnetic excitation spectrum was observed at $T = 5$ K. One of the significant features is the flat excitations around 4.5 meV with an intense spot around 1 Å^{-1}. As demonstrated in Figs. 3(c)–3(e), we performed linear spin-wave calculations using SPINW [14] on the spin Hamiltonian below by assuming two magnetic models of 3PD state with spin anisotropy $S \parallel c$ and the 120° structure with $S \parallel ab$ plane:

$$H = \sum_{n=1}^{3} J_n \sum_{<i,j>} S_i S_j + J_c \sum_{<i,j>} S_i S_j + D_c \sum_i S_z^2 i.$$

Here, the J_n ($n = 1, 2, 3$) is the in-plane nearest, second, and third neighbor interactions, J_c is the interplane nearest neighbor interaction, D_c is the single-ion anisotropy representing an effective Ising (negative sign) or XY (positive sign) anisotropy, and S_i and S_j are spins at sites i and j corresponding to the relevant couplings J_n and J_c. The calculations for the 3PD state with the spin anisotropy $S \parallel c$ reproduce the overall feature of the magnetic excitations with $J_1 = 5.1$ K, $J_2 = 0.51$ K, $J_3 = 2.6$ K, $J_c = 0$ K, $D_c = -1.2$ K (model I) for Fig. 3(c) and $J_1 = 4.9$ K, $J_2 = 0.49$ K, $J_3 = 2.5$ K, $J_c = 0.8$ K, $D_c = -1.2$ K (model II) for Fig. 3(d). Including a finite out-of-plane interaction J_c, the excitations around 4.5 meV become broader. The broadening of the spin-wave modes is also driven due to the short-ranged spin correlations, which we believe would be the primary cause of the very broad excitations observed. We also found that further neighbor interactions J_2 and J_3 are required to explain the Q dependence of the intensity around 4.5 meV, as shown in Fig. 3(f). We can apparently rule out the 120° structure [model III, Fig. 3(e)], which is a well-known candidate as a ground state of the classical triangular antiferromagnet.

The estimation of the magnetic interactions enables us to gain an insight into the magnetic system of Ag_2FeO_2. The ratio of the in-plane nearest neighbor and interplane interaction is $J_c/J_1 = 0.16$ using the set of interactions for model II. This indicates that Ag_2FeO_2 is two-dimensional magnetic system which is consistent with the structural feature of the compound. The degree of anisotropy is comparable to that of $CuFeO_2$ as a possible Ising Fe^{3+} compound by comparing it in the unit of D/J_1; $D/J_1 = -0.24$ for Ag_2FeO_2 using J_1 for the 3PD models and $D/J_1 = -0.17$ [15] to -0.35 for $CuFeO_2$ [16]. The origin of this Ising anisotropy has not been completely understood yet. However, one scenario was proposed by Wang *et al.*, in which the spin-lattice coupling effect stabilized the Ising spin anisotropy even in the orbital quenched system [17]. This mechanism was applied to explain the anisotropy of $CuFeO_2$. We consider this as the possible case of Ising anisotropy of our compound.

The obtained inelastic scattering spectrum is qualitatively similar to that of the collinear antiferromagnetic ordered state of honeycomb antiferromagnets, which is consistent with the emergence of the 3PD state. The broadening of the observed spectrum is probably caused by the short-ranged spin correlation and the finite interplane coupling. Importantly, this set of the magnetic interactions with large further neighbor interactions on triangular lattice stabilizes the 3PD state, comparing with the calculated magnetic phase diagram for the classical Ising triangular antiferromagnet [18].

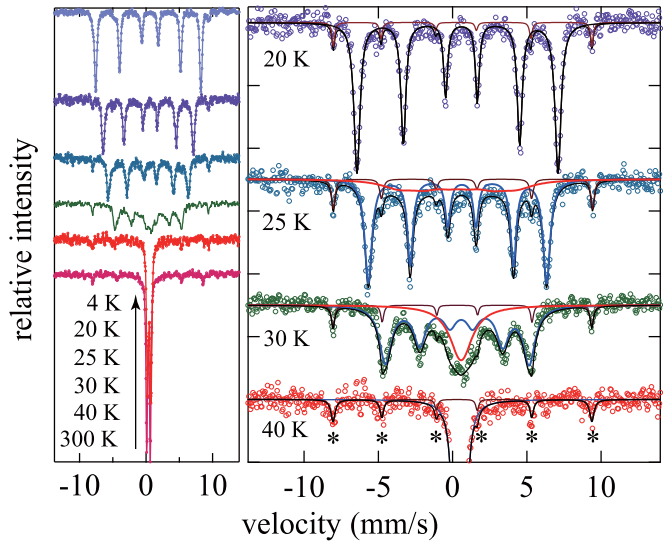

FIG. 4. Mössbauer spectra of Ag_2FeO_2. The circles are our experimental data. The black line is the result of the fitting. The right panel is a magnified plot. The asterisks indicate the impurity (Fe_2O_3) signal. The spectra at 30 and 25 K are divided into two components: C-1 (blue line) and C-2 (red line).

Figure 4 shows the results of ^{57}Fe Mössbauer measurements. Spectra above 40 K ($>T_p$) indicate the presence of a paramagnetic state. At 300 K, the isomer shift is 0.36 mms^{-1}, and the quadrupole splitting is 0.54 mms^{-1}. Critical behavior was observed in the intermediate temperature range ($T_c < T < T_p$). The right panel of Fig. 4 is a magnified plot of the region from 20 to 40 K. At 30 and 25 K, complicated splitting of the spectrum is observed; the spectra consists of two components, C-1 and C-2. At 30 K, the component C-1 is a sextuplet with an internal field $H_{int1} \approx 30$ T and a volume fraction $V_{m1} \approx 65\%$. The C-2 is represented as a broad central structure approximated by the sextuplet with $H_{int2} \approx 0$ T and $V_{m2} \approx 28\%$, which suggests that the C-2 spins behave like a paramagnet at this temperature. At 25 K, C-1 is characterized by $H_{int1} \approx 37$ T and $V_{m1} \approx 66\%$, and C-2 shows a broadening which is fitted by the sextuplet with $H_{int2} \approx 24$ T and $V_{m2} \approx 25\%$. The ratio of the volume fractions between C-1 and C-2 is close to 2:1 at 25 and 30 K, which is one of the significant feature of the intermediate temperature phase. This is consistent with the 3PD structure determined by neutron experiments.Therefore, C-1 can be assigned to an ordered spin component, whereas C-2 is thought to be a disordered spin component. Below 20 K ($<T_c$), the spectra are unified into one sextuplet with $H_{int} \approx 42$ T at 20 K and $\approx$49 T at 4 K, indicating that the spins form an ordered state.

IV. DISCUSSION

These experiments revealed that exotic successive magnetic anomalies appeared at T_p and T_c. T_p represents a

second-order phase transition, whereas T_c should be a crossover phenomenon evidenced by the broad feature in the magnetic heat capacity. First, we consider the magnetic state of the intermediate phase. The magnetic structure of the intermediate phase is expected to be the 3PD state based on the Mössbauer and neutron scattering experiments. The Mössbauer study clearly revealed that the internal field H_{int1} appeared just below the magnetic phase transition at T_p. On the other hand, no internal field is observed for C-2 spin components at the same time. This indicates that one third of spins sit on the spin sites where the internal field cancels out. Interestingly, the disordered spins start to be influenced by H_{int2} below T_p, suggesting that fluctuation of the disordered spins slows down with decreasing temperature. H_{int2} is detectable below ≈25 K because its frequency becomes comparable to the characteristic time scale of Mössbauer spectroscopy. This effect implies that the disordered spins in the PD state are not completely equivalent to free paramagnetic spins as theoretical PD model but correlate with the ordered spins through magnetic interaction.

Second, we consider the ground-state properties of Ag_2FeO_2. The occurrence of successive transitions implies that the magnetic state below T_p changes to form a different magnetic state as suggested by the entropy release around T_c, although the modification of magnetic structure has not been detected experimentally. A representative theory for the classical Heisenberg-Ising triangular antiferromagnet provides a hint of the magnetic behaviors of Ag_2FeO_2. It predicted that the occurrence of the successive magnetic phase transitions where the PD phase appeared at higher transition temperature, and 120° LRO developed at lower transition temperature [19]. The difference between experimental results and theoretical predictions is that the Ag_2FeO_2 does not show the LRO even at the lowest temperature based on the short spin correlation length. As temperature decreases, the spin correlation length ξ increases throughout the intermediate temperature range ($T_c < T < T_p$), accompanied by a critical slowdown of the fluctuation of the disordered spins. At T_c, ξ reaches a finite value and maintains it down to the lowest temperature. This means that the magnetic state below T_c is not a conventional long-range ordered state. The saturation of ξ suggests that the spin fluctuation is not completely reduced at low temperature. We presume that the spins slowly fluctuate below T_c because of a quantum instability enhanced by the magnetic frustration.

A similar phenomenon was reported by Olariu *et al.* for $NaCrO_2$, an $S = 3/2$ Heisenberg TAFM [20]. They showed that there is a high-temperature peak in the specific heat, whereas the divergence of μSR T_1^{-1} occurs only at a lower temperature. In the intermediate-temperature range, there are still spins fluctuating rapidly; they slow down at lower temperatures, a result similar to the one found in the present study. Kawamura *et al.* theorized the presence of a "spin-gel" state below the characteristic temperature T_v with finite spin correlation length in Heisenberg TAFMs [21]. Their calculations are in good agreement with results reported for $NaCrO_2$. Although it is not unclear whether their theory is applicable to the phenomenon observed in Ag_2FeO_2 or not, interesting physics relating to the magnetic frustration is observed on the classical triangular lattice.

Another possibility is the sequential magnetic behaviors as observed in $GdInCu_4$ [22]. $GdInCu_4$ crystalizes in the cubic C15 type structure which exhibits the successive anomalies at $T_N = 7$ K and $T_M = 3.5$ K. Just below T_N, an unusual PD state is realized in this compound where spins on the certain layer perpendicular to $[0, k, 0]$ direction show the Néel-type antiferromagnetic order and the spins on the adjacent layer behave paramagnetically. Below T_M, the paramagnetic spins freeze at all once. The magnetic properties of $GdInCu_4$ are similar to those of Ag_2FeO_2 at a glance. However, no magnetic diffuse scattering in neutron diffraction, no hysteresis between FC and ZFC process in magnetic susceptibility were observed in Ag_2FeO_2 which are characteristic feature of $GdInCu_4$ scenario. Significantly, the magnetic dimensionality affects the magnetic behaviors of each compound; Ag_2FeO_2 is a good 2D magnet and $GdInCu_4$ is considered to be a 3D magnet. Since Ag_2FeO_2 is the 2D antiferromagnet, the magnetic state where all spins on a certain layer behave as paramagnet suffer a significant loss of the in-plane exchange interaction. These facts qualitatively suggest that the magnetic properties of both compounds are caused by different origins.

At present, the following two questions remain: "Why the short-range spin correlation state does exist in the Ising-like spin system?" and "Is the PD state a proper ground state of Ag_2FeO_2?" In order to clarify the magnetic properties of Ag_2FeO_2, further microscopic experiments are necessary. Furthermore, theoretical studies should be revisited to better understand the physics of the strong Ising-spin case of classical TAFMs.

V. CONCLUSIONS

In conclusion, we have successfully synthesized an $S = 5/2$ classical triangular antiferromagnet Ag_2FeO_2. We found an exotic phase transition at $T_p = 36$ K and a crossover phenomenon around $T_c = 20$ K. Below T_p, a three-sublattice partially disordered state was observed. Below T_c, spins form a slowly fluctuating state in which the 3PD structure persists and the spin correlation length remains short. To clarify the magnetic properties of Ag_2FeO_2, further theoretical and experimental studies are required.

ACKNOWLEDGMENTS

We are grateful to M. Oda (Hokkaido University) and N. Hayashi (Kyoto University) for the fruitful discussions. We thank S. E. Dissanayake for letting us use a code for powder averaging dispersions on SPINW. This research was partly supported by Grants-in-Aid for Scientific Research from the JSPS (Grants No. 22-10454, No. 18K03529, No. 22560676, and No. 22246083). This research used resources at the High Flux Isotope Reactor and Spallation Neutron Source, which are DOE Office of Science User Facilities operated by the Oak Ridge National Laboratory.

[1] G. H. Wannier, Phys. Rev. **79**, 357 (1950).
[2] K. Wada and T. Ishikawa, J. Phys. Soc. Jpn. **52**, 1774 (1983).
[3] S. Miyashita and H. Shiba, J. Phys. Soc. Jpn. **53**, 1145 (1984).

[4] D. H. Lee, J. D. Joannopoulos, J. W. Negele, and D. P. Landau, Phys. Rev. B **33**, 450 (1986).
[5] H. Kawamura and S. Miyashita, J. Phys. Soc. Jpn. **53**, 9 (1984).
[6] M. Schreyer and M. Jansen, Angew. Chem. **41**, 643 (2002).
[7] H. Yoshida, Y. Muraoka, T. Sorgel, M. Jansen, and Z. Hiroi, Phys. Rev. B **73**, 020408(R) (2006).
[8] D. L. Abernathy, M. B. Stone, M. J. Loguillo, M. S. Lucas, O. Delaire, X. Tang, J. Y. Y. Lin, and B. Fultz, Rev. Sci. Instrum. **83**, 15114 (2012).
[9] M. Onoda, J. Crystallogr. Soc. Jpn. **46**, 407 (2004).
[10] See Supplemental Material at http://link.aps.org/supplemental/10.1103/PhysRevResearch.2.043211 for more information about the structural analysis incorporating the stacking fault of the title compound.
[11] H. Yoshida, S. Ahlert, M. Jansen, Y. Okamoto, J. Yamaura, and Z. Hiroi, J. Phys. Soc. Jpn. **77**, 074719 (2008).
[12] M. Mekata, J. Phys. Soc. Jpn. **42**, 76 (1977).
[13] S. Fujiki, K. Shutoh, and S. Katsura, J. Phys. Soc. Jpn. **53**, 1371 (1984).
[14] S. Toth and B. Lake, J. Phys.: Condens. Matter **27**, 166002 (2015).
[15] F. Ye, J. A. Fernandez-Baca, R. S. Fishman, Y. Ren, H. J. Kang, Y. Qiu, and T. Kimura, Phys. Rev. Lett. **99**, 157201 (2007).
[16] T. Nakajima, A. Suno, S. Mitsuda, N. Terada, S. Kimura, K. Kaneko, and H. Yamauchi, Phys. Rev. B **84**, 184401 (2011).
[17] F. Wang and A. Vishwanath, Phys. Rev. Lett. **100**, 077201 (2008).
[18] T. Takagi and M. Mekata, J. Phys. Soc. Jpn. **64**, 4609 (1995).
[19] S. Miyashita and H. Kawamura, J. Phys. Soc. Jpn. **54**, 3385 (1985).
[20] A. Olariu, P. Mendels, F. Bert, B. G. Ueland, P. Schiffer, R. F. Berger, and R. J. Cava, Phys. Rev. Lett. **97**, 167203 (2006).
[21] H. Kawamura, A. Yamamoto, and T. Okubo, J. Phys. Soc. Jpn. **79**, 023701 (2010).
[22] H. Nakamura, N. Kim, M. Shiga, R. Kmiec, K. Tomala, E. Ressouchek, J. P. Sanchezk, and B. Malaman, J. Phys.: Condens. Matter **11**, 1095 (1999).